

# Development and characterization of novel hydrogel containing antimicrobial drug for treatment of burns

Vaishali Thakkar, Vaishali Korat, Lalji Baldaniya, Mukesh Gohel, Tejal Gandhi, Nirav Patel<sup>1</sup>

Department of Pharmaceutics, Anand Pharmacy College, Anand, <sup>1</sup>Department of Pharmaceutical Sciences, Saurashtra University, Rajkot, Gujarat, India

## Abstract

**Introduction:** The aim of burn management and therapy is fast healing and epithelisation to prevent infection. The present study is concerned with the development and characterization of a novel nanaoparticulate system; cubosomes, loaded with silver sulfadiazine (SSD) and Aloe vera for topical treatment of infected burns. **Methods:** Cubosome dispersions were formulated by an emulsification technique using different concentrations of a lipid phase Glyceryl Monooleate (GMO) and Poloxamer 407. The optimum formulae were incorporated in an aloe vera gel containing carbopol 934, to form cubosomal hydrogels (cubogels). The cubogels were characterized by *in vitro* release of SSD, rheological properties, pH, bioadhesion, Transmission Electron Microscopy and *in-vivo* Wound Healing Study. **Results:** The results show that the different concentration of GMO had significant effect on particle size, % EE and *in vitro* drug release. From the *in-vitro* drug release pattern and similarity factor ( $f_2$ ), it was concluded that batch CG3 (15% GMO and 1% P407) exhibited complete and controlled drug release within 12 hour (i.e. 98.25%), better bio adhesion and superior burn healing as compared to the marketed product. **Conclusion:** The *in vivo* burns healing study in rats revealed that the prepared optimized cubogel containing SSD and aloe vera has superior burns healing rate than cubogel with only SSD and marketed preparation so, it may be successfully used in the treatment of deep second degree burn.

**Key words:** *Aloe vera*, cubogel, histopathological study, *in vivo* burns healing, novel nanaoparticulate system, silver sulfadiazine

## INTRODUCTION

A burn is the most serious skin or other organic tissue injuries mainly caused by heat, radiation, radioactivity, electricity, friction, or contact with chemicals. The other causes of skin injuries are due to ultraviolet radiation, radioactivity, electricity or chemicals, and respiratory damage resulting from smoke inhalation, which are also considered as burns. Globally, burns are a serious public health problem, and it estimated 195,000 deaths occur each year from fires alone, with more deaths from scalds, electrical burns, and other forms of burns.<sup>[1]</sup> The main goal of burn management and therapy is to prevent infection by providing quicker healing and formation of epithelium over a denuded surface.<sup>[2]</sup> The

survival of patients with major burns by minimizing the chances of burn wound sepsis and healing with the least amount of scarring is the ultimate goal for all topical therapy.<sup>[3]</sup>

One of the most widely used treatments for the topical burn is silver sulfadiazine (SSD), the most well-known topical antibacterial agent for the treatment of burns. It is on the World Health Organization's List of Essential Medicines, a list of the most important medication needed in a basic health system. It combines the inhibitory action of silver salt along with the antibacterial effect of sulfadiazine. Silver has an effective antimicrobial with broad Gram-negative and Gram-positive activities, antifungal properties as well as potent anti-inflammatory properties. The inhibitory action of silver is due to

### Address for correspondence:

Dr. Nirav Patel,  
Department of Pharmaceutical Sciences, Saurashtra University,  
Rajkot - 360 005, Gujarat, India.  
E-mail: nirav2564@gmail.com

### Access this article online

Quick Response Code: 	Website: <a href="http://www.jpionline.org">www.jpionline.org</a>
	DOI: 10.4103/2230-973X.187343

This is an open access article distributed under the terms of the Creative Commons Attribution-NonCommercial-ShareAlike 3.0 License, which allows others to remix, tweak, and build upon the work non-commercially, as long as the author is credited and the new creations are licensed under the identical terms.

**For reprints contact:** [reprints@medknow.com](mailto:reprints@medknow.com)

**How to cite this article:** Thakkar V, Korat V, Baldaniya L, Gohel M, Gandhi T, Patel N. Development and characterization of novel hydrogel containing antimicrobial drug for treatment of burns. *Int J Pharma Invest* 2016;6:158-68.

its strong interaction with thiol groups present in the bacterial cell respiratory enzymes. It also interacts with structural proteins and inhibits replication by preferentially binding with DNA bases.<sup>[4-7]</sup>

The current carrier (commercially available cream, ointment, paste) of SSD possesses many disadvantages such as wrinkling, allergic reactions, drying of wound, takes more time, not generate skin as natural skin, not easy to wash out, etc. It also forms an adhesive pseudoeschar which may hinder the penetration of SSD into the burn wound.<sup>[8,9]</sup> The antibacterial action of SSD is due to heavy metals, and it also produces toxicity toward fibroblasts and keratinocytes.<sup>[10,11]</sup> *In vitro* studies showed that SSD is cytotoxic, but its cytotoxicity can be minimized by controlling its releases from the dosage form, which may be achieved by formulating novel cubogel.<sup>[12,13]</sup>

Cubogels are the cubosomal dispersion of hydrogel. Hydrated polymer (hydrogel) dressings, originally developed in the 1950s, contain 90% water in a gel base, which helps regulate fluid exchange from the wound surface. Hydrogel dressing is usually clear or translucent and differs in viscosity or thickness. By providing moisture to the wound, hydrogel dressings create a moist healing environment, which promotes granulation, epithelialization, and autolytic debridement. The high water content of hydrogel dressings cools the wound, producing pain relief effect that can last up to 6 h, and contribute to their biocompatibility. Dressing-change discomfort is also reduced because hydrogels don't adhere to the wound surface because of low interfacial tension between the hydrogel surface and the body fluid. Hydrogels may provide desirable protection of drugs, peptides, and especially proteins from the potentially harsh environment in the vicinity of the release site. In summary, hydrogel dressings give soothing effect and reduce pain, rehydrate the wound bed, facilitate autolytic debridement, fill in dead space, and can be used when the infection is present.<sup>[14-17]</sup>

Cubosomes are nanosized structures formed by dispersion of bicontinuous cubic liquid crystalline phases. The self-assembled nanostructured materials are used for controlling the release of incorporated drugs which are recent trends in drug delivery. In the pharmaceutical area, viscous lipid-based systems such as bicontinuous cubic liquid crystalline phases, offer considerable scope for application as drug delivery systems as these nanoparticles are dispersions of liquid crystalline phases in excess water. Cubic-Phase Nanoparticles or cubosomes are liquid crystalline nanoparticles with the same unique properties of the bulk cubic phase; conversely, cubosome dispersions have much lower viscosity.<sup>[18-20]</sup>

Glyceryl monooleate (monoolein or GMO), a polar lipid, is a nontoxic, biodegradable, and biocompatible material classified as generally recognized as safe and included in the Food and Drug Administration (FDA) inactive ingredients guide. The bicontinuous cubic phase of GMO has several attractive features like biodegradable because of GMO is an object of lipolysis, able to solubilize water-soluble, oil-soluble, and amphiphilic substances

within its aqueous and lipid domains and release of these substances in a controlled manner with the suitable organization of the bicontinuous cubic liquid crystals and also has mucoadhesive property.<sup>[21-23]</sup> *Aloe vera* is a photosynthetic plant of great interest for several biomedical and pharmaceutical preparations due to its therapeutic properties. Several therapeutic properties have been assigned to the *A. vera* gel including antibacterial, antiseptic, anti-inflammatory, and ability to stimulate the proliferation of fibroblasts and the synthesis of collagen.<sup>[24,25]</sup> *A. vera* gel is used in concert with SSD for obtaining a quicker clinical response.

In the light of above facts, the aim of this present investigation deals with the development and characterization of SSD loaded cubosomes followed by incorporation of cubosomes into an *A. vera* hydrogel. The prepared cubogels have been evaluated *in vitro* and their wound healing activity is also evaluated by an *in vivo* animal model.

## MATERIALS AND METHODS

### Materials

SSD was kindly supplied as a gratis sample by Bharat Parenteral, Baroda, Gujarat, India and GMO by Chemdyes Corporation, Rajkot. Polyvinyl alcohol, carbopol 934, carbopol 940, and propyl paraben sodium salt and triethanolamine were obtained from Loba chemie Pvt Ltd., (Mumbai, India). Poloxamer 407 was purchased from BASF chemical company (Mumbai). Di-sodium ethylenediaminetetraacetic acid (EDTA), sodium benzoate, Methylparaben, dist. Water, triethanolamine, ammonia, ammonium phosphate, disodium hydrogen phosphate, potassium dihydrogen phosphate, sodium sulfate, sodium chloride, and methanol were purchased from SD Fine Chemicals, Mumbai. *A. vera* gel was supplied by Vasu pharmaceutical, Baroda.

### Preparation silver sulfadiazine loaded cubosome

Production of cubosomal dispersions was based on the emulsification of monoglyceride/surfactant mixture in water. The composition of various formulations is presented in Table 1. Poloxamer 407 was used as surfactant in a concentration range of 0-2% w/w and the lipid based self-assembling monoglyceride (GMO) was used in the concentration range of 0-30% w/w. GMO was melted on a water bath at 70°C, and poloxamer 407 was dissolved into dist. water at 70°C separately. The aqueous

**Table 1: Composition of cubosomal dispersion**

Formulation	GMO (%)	Poloxamer 407 (%)	Water (mL)
CS1	5	0.5	94.50
CS2	15	0.5	84.50
CS3	25	0.5	74.50
CS4	5	1.0	94.00
CS5	15	1.0	84.00
CS6	25	1.0	74.00
CS7	5	2.0	93.00
CS8	15	2.0	83.00
CS9	25	2.0	73.00

Each batch contains 1% of SSD, GMO: Glyceryl monooleate, SSD: Silver sulfadiazine

solution containing dissolved poloxamer 407 was added dropwise into a molten mixture of GMO at the same temperature under mechanical stirring (Remi Equipment, Ms-500, Mumbai, India) at 1500 rpm for 2 h. The dispersion was allowed to cool at room temperature. After emulsification, the dispersion was subjected to ultra-sonication (Sartorius, LABSONIC M) at 5 amplitude for 15 min. Cubosomal dispersions were stored at room temperature.<sup>[26-28]</sup>

### Characterization of cubosomal dispersion

#### Entrapment efficiency

The cubosomes from the resulting dispersions were first separated by centrifugation. The separation of the free (nonentrapped) drug from the entrapped drug in the cubosome dispersion was achieved by centrifugation at 8000 rpm for 15 min. The supernatant liquid was separated and diluted.<sup>[29,30]</sup> The amount of free drug in the dispersion was then analyzed spectrophotometrically at  $\lambda_{max}$  254.7 nm which was then subtracted from the total amount of drug initially added. Each experiment was repeated 3 times. The % entrapment efficiency (EE) was calculated by the following equation:

$$\% \text{ of EE} = \frac{C_t - C_f}{C_t} \times 100$$

where,

$C_t$  is equal to total drug concentration,

$C_f$  is equal to free drug concentration.

#### Particle size and zeta potential measurement

Particle size and zeta potential were determined using photon correlation spectroscopy on a Malvern Zetasizer 3000 (Malvern Instruments, Malvern, UK) at 25°C assuming a viscosity of pure water and presented as an average of three separate determinations. The zeta potential is an indication of the stability of the colloidal systems and indicates charge present on the particles of the colloidal systems.<sup>[31]</sup> Samples were placed in clear disposable zeta cells, and results were recorded. Before putting the fresh sample, cuvettes were washed with the methanol and rinsed using the sample to be measured before each experiment.

#### Visual examination of phase separation of cubosomal dispersion

The initial stability of dispersions was assessed visually through observation of the samples in the sample wells after sonication. A well-dispersed sample contained no visible aggregates and possessed a milky white consistency. In contrast, poorly dispersed samples were largely transparent systems with visible aggregates of lipid typically around the rim of the sample well. The visual assessment was used as an initial screen to rapidly exclude very poor dispersions from further study.<sup>[31,32]</sup>

#### Optical microscopy and cryo-transmission electron microscopy

An optimized batch of the cubogel was viewed under a light microscope with a two-dimensional camera to study their cubic shape and lamellarity. The cubogel will suitably diluted, then

the diluted solution was deposited on a glass slide and observed by light microscope under magnification of  $\times 400$ . Cryo-transmission electron microscopy (TEM) was used to check the morphology and confirm the formation of cubic structures in the prepared cubosome dispersions. Samples were prepared at ambient conditions. A 10-ml drop of solution was placed on a pure thin bar 600-mesh TEM grid (Model Philips Tecnai 20, Holland). The drop was blotted with filter paper until it was reduced to a thin film (10-200 nm) spanning the hexagonal holes of the TEM grid. The sample was then vitrified by rapidly immersing into liquid ethane near its freezing point. The vitrified specimen was transferred to a Zeiss EM922 transmission electron microscope for imaging using a cryoholder. The temperature of the sample was kept below  $-175^\circ\text{C}$  throughout the examination. Specimens were examined with doses of about 1000-2000 e/nm<sup>2</sup> at 200 kV. Images were recorded digitally by a charge coupled device camera (Ultrascan 1000, Gatan) using an image processing system (GMS 1.4 software, Gatan).<sup>[33]</sup>

#### Preparation of Aloe vera hydrogel

From the results of preliminary studies, it can be concluded that carbopol 934 is a good gelling agent for *A. vera* gel hydrogel. The *A. vera* hydrogel was prepared by dispersing carbopol 934 into an *A. vera* gel using a magnetic stirrer. Other excipients were dissolved in solution after the uniform dispersion of carbopol 934. The pH of resulting solution was adjusted by triethanolamine. Four different batches of *A. vera* hydrogel were prepared that contained 0.5, 1, 1.5, and 2% of carbopol 934. The composition of the formulation is depicted in Table 2. The prepared *A. vera* hydrogel were characterized for various parameters.

#### Preparation of Aloe vera based silver sulfadiazine cubogel

Cubosome dispersion containing a different concentration of GMO from 5% to 30% w/w with 1% w/w of poloxamer 407 was prepared by emulsification as mentioned above. The composition of cubosome loaded *A. vera* hydrogel is depicted in Table 3. Cubosome loaded *A. vera* hydrogel was prepared by sprinkling carbopol 934 (1.5% W/V) over *A. vera* gel (75% V/V) and stirred using magnetic stirrer. Sodium benzoate, methylparaben, and disodium EDTA were added after the complete dispersion of carbopol 934. At the same time, cubosomal dispersion (CG1-CG6) was added and stirred with a magnetic stirrer. pH was adjusted by triethanolamine that led to the formation of a white creamy hydrogel.<sup>[34,35]</sup>

**Table 2: Composition of *A. vera* hydrogel containing carbopol 934 as gelling agent**

Ingredients	Batches			
	HG1	HG2	HG3	HG4
<i>A. vera</i> gel (%)	75	75	75	75
Carbopol 934 (%)	0.5	1.0	1.5	2.0
Methyl paraben (%)	0.2	0.2	0.2	0.2
Disodium EDTA (%)	0.1	0.1	0.1	0.1
Sodium benzoate (%)	0.4	0.4	0.4	0.4

EDTA: Ethylenediaminetetraacetic acid, *A. vera*: *Aloe vera*

**Table 3: Composition of *A. vera* based SSD cubogel**

Ingredients (%)	Formulation code					
	CG1	CG2	CG3	CG4	CG5	CG6
SSD	1	1	1	1	1	1
GMO	5	10	15	20	25	30
Poloxamer 407	1	1	1	1	1	1
<i>A. vera</i> gel	75	75	75	75	75	75
Carbopol 934	1.5	1.5	1.5	1.5	1.5	1.5
Sodium benzoate	0.4	0.4	0.4	0.4	0.4	0.4
Disodium EDTA	0.1	0.1	0.1	0.1	0.1	0.1
Methylparaben	0.2	0.2	0.2	0.2	0.2	0.2
Distilled water	Q.S.	Q.S.	Q.S.	Q.S.	Q.S.	Q.S.

SSD: Silver sulfadiazine, GMO: Glycerol monooleate, EDTA: Ethylenediaminetetraacetic acid, *A. vera*: *Aloe vera*

### Characterization of *Aloe vera* based silver sulfadiazine cubogel

#### Drug entrapment efficiency

The drug EE of cubogel was measured same as like cubosome which is described in the previous section.<sup>[29,30]</sup>

#### Measurement of bioadhesion

The bioadhesive force of cubogel was measured on a modified physical balance. The membrane used for bioadhesion testing was Rat intestinal microvillus membranes. The membrane was fitted on the glass stage using an adhesive tape. Very thin layer of each cubogel was applied in 2 cm disks of aluminum foils attached to the balance pan. A preload of 50 g was applied to the balance pan above aluminum disks for 5 min then removed. The weights were increased until the dermal tissue, and the cubogel thin film backed by the aluminum foil became detached. The weight required to detach the tissue from cubogel thin film was taken as a measure of the bioadhesive strength.<sup>[36-38]</sup> The bioadhesive force was determined using the following equation:

$$\text{Force of adhesion} = \text{Bioadhesive strength} \times 98.1/100$$

#### Rheological properties of *Aloe vera* based silver sulfadiazine cubogels

Brookfield Viscometer, (Model DV II+ Pro) with helipath stand, was used for rheological studies. The sample (30 g) was placed in a beaker and was allowed to equilibrate for 5 min before measuring the dial reading using a T-C spindle at 0-100 rpm of angular velocity. At each speed, the corresponding dial reading on the viscometer was noted. The T-C spindle was successively lowered, and the corresponding dial reading was noted.<sup>[39]</sup> The measurements were performed in triplicate and the mean viscosity of the all batch was calculated.

#### In vitro drug diffusion study

The Franz diffusion cell was used for studying the *in vitro* release of SSD from the cubosome loaded hydrogel. A cellulose acetate membrane (Himedia Dialysis membrane-110 with 21.5 mm diameter) was adapted to the terminal portion of the cylindrical donor compartment. 30 mg equivalent drug portion of hydrogel was placed in the donor compartment. The receptor compartment

contained 15 ml of phosphate buffer solution of pH 6.8. The buffer was maintained at 37°C under mild agitation using a magnetic stirrer. At specific time intervals 0.5, 1, 2, 3, 4, 5, 6, 7, 8, 10, 12 h aliquots of 1 mL were withdrawn and immediately restored with the same volume of fresh phosphate buffer.<sup>[38,39]</sup> The amount of drug released was assessed by measuring the absorbance at 254.7 nm using an ultraviolet spectrophotometer.

#### J flux calculation

The *in vitro* diffusion study for the gels was carried out by using diffusion cell which was opened at both the ends. The mean cumulative amount of drug permeated per unit surface area was plotted versus time. The slope of the linear portion of the plot was calculated as flux  $J$  (mg/cm/h), and the permeability coefficient was calculated using equation,

$$K_p = J/C_d,$$

Where,  $K_p$  is the permeability coefficient

$C_d$  is the initial drug concentration in drug compartment.

#### Kinetics of drug release

The drug release kinetics was studied by plotting the data obtained from *in vitro* release in various kinetic models like zero order, first order, Korsmeyer's-Peppas, and Higuchi.<sup>[40]</sup>

#### In vivo wound healing study

The preclinical study protocol for burns healing study in rats was approved by the Institutional Animal Ethical Committee, Anand Pharmacy College, Anand (protocol no. 1328). Male Wistar rats weighing approximately 250 g were anesthetized with phenobarbital i.p. The skins of the animals were shaved and disinfected using 70% ethanol. Two full thickness skin wounds of 1 cm<sup>2</sup> area were prepared by excising the dorsum of the animals by a metal rod (1.5 cm diameter) heated to 80-85°C and exposed for 20 s. Rats were divided into four groups of 6 animals each. After creating two full thickness wound areas (1 cm × 1 cm) by excising the dorsum, 70% ethanol was used for sterilization. The animals of group I were untreated and considered as the control, group II served as reference standard (SSD cream), animals of group III, and IV were treated with the cubogel without drug and the cubogel with drug (test). The reference standard, cubogel without drug, and test were applied topically on wound twice a day, starting from the day of burn wound induction. All rats were separately kept in individual cages. At the 0, 3<sup>rd</sup>, 6<sup>th</sup>, 9<sup>th</sup>, 12<sup>th</sup> days after the operation, the wound area was traced manually on a glass slide and photographed. % wound closure was calculated using the following a formula.<sup>[41-44]</sup>

$$\% \text{ wound closure} = \frac{\text{Wound area on day 0} - \text{Wound area on day } n}{\text{Wound area on day 0}} \times 100$$

#### Histopathological examination

Autopsy samples were taken from the skin of rats in different groups and fixed in 10% formol saline for 24 h. Washing was

done with distilled water, and then, serial dilutions of absolute ethyl alcohol were used for dehydration. Specimens were cleared in xylene and embedded in paraffin at 60°C in a hot air oven for 24 h. Paraffin beeswax tissue blocks were prepared for sectioning at 4 µm by sledge microtome. The obtained tissue sections were collected on glass slides, deparaffinized, and stained with hematoxylin, and eosin stains for histopathological examination through the electric light microscope.<sup>[45]</sup>

### Stability study

To assess the drug and formulation stability, stability study was done for 3 months. Optimized formulation was kept in a humidity chamber maintained at 40°C and 75% relative humidity (RH) for the suitable time period. The sample was analyzed for the physical appearance, pH, viscosity, and % of EE.

## RESULTS AND DISCUSSION

### Characterization of cubosomal dispersion

#### Drug entrapment efficiency (%), particle size and zeta potential measurement

Drug EE was determined in order to make sure that the added amount of SSD is present in the cubosome dispersion. The EE of all batches is in the range of 74.93 ± 0.903-92.10 ± 0.250 as shown in Table 4. The highest EE was found in the batch CS5, consisted of 15% of GMO, and 1% of poloxamer 407. The EE of SSD into cubic nanoparticles was dependent on the concentration of GMO and poloxamer 407. The result showed that the EE increased, as the amount of lipid and surfactant increased. Increasing amount of GMS was bound to increase the % of EE because of the increased concentration of mono-, di-, and triglycerides, which act as solubilizing agents for SSD and provide more space to accommodate excessive drugs. This effect may be observed due to the increased viscosity of the medium, because increasing the amount of lipid resulted in faster solidification of the cubosomal nanoparticles, which would prevent drug diffusion to the external phase of the medium. As the percentage of emulsifier increased, part of the SSD was incorporated in the surfactant layer at the surface of the cubosomes, leading to a high entrapment efficacy.

The particle size and zeta potential affects the biopharmaceutical, physicochemical, drug release, and stability of the cubosomal

nanoparticles. The result showed that as the GMO content increases, the particle size decreases. Zeta potential values of cubosomal dispersion were dependent on the ratios of GMO/P407. The lower zeta potential value in this study is due to nonionic surfactant, it stabilizes the system by a steric hindrance to avoid aggregation during storage. The zeta potential was found to be lower in Batches CS4-CS6, that is, formulations containing 1% poloxamer 407 which indicates high negative surface charge on cubosomes which in turn indicates higher stability because of the anticipated surface repulsion between similar charged particles. It was known that the particle size distribution was one of the most important characteristics for evaluation of the stability of colloidal systems.<sup>[30]</sup> The mean particle size (z-ave) and the zeta potential were measures to evaluate the width of the size distribution and measure of overall charges acquired by particles in a particular medium and is considered as one of the benchmarks of stability of the colloidal system.<sup>[31]</sup> Table 4 shows the particle size distribution and zeta potential of all batches which are in the range of 193.6-432.0 nm and -17.61 to 7.41, respectively. Figure 1 shows the particle size analysis of batch CS5. Figure 2 shows that the cubosomal dispersion is physically stable at 1% of poloxamer concentration.

### Visual examination of phase separation of cubosomal dispersion

The initial stability of dispersions was assessed visually through physical observation of the samples in the vials after sonication. The results of phase separation are represented in Figure 2. The phase separation was observed in batches CS1-CS3 and CS7-CS9 whereas, batches CS4-CS6 were found to be physically stable. The visual assessment was used as an initial screen to rapidly exclude very poor dispersions from further study. Hence, batches with 0.5% and 2.0% poloxamer 407 were rejected, while poloxamer 407 (1%) produced stable cubosomal dispersion and selected for further study.

### Optical microscopy of cubosomal dispersion

The optimized batch of cubosome dispersion was observed under a light microscope at ×40. From the photomicrograph [Figure 3], it indicates that the cubosomes are well separated from each other. Though this study, it does not give any exact estimate of the cubic shape of vesicle, so cryo-TEM was done to confirm its morphology. The optimized batch of

**Table 4: Percentage of EE and particle size and zeta potential of cubosome dispersion**

Batches	EE (%)	Particle size (nm)	Zeta potential (mV)
CS1	74.93±0.903	283.7	-0.69
CS2	78.62±0.304	246.0	-10.9
CS3	78.50±1.205	237.6	-8.59
CS4	80.65±0.383	197.7	-13.46
CS5	92.10±0.250	193.6	-11.16
CS6	90.06±0.460	190.5	-17.61
CS7	78.826±0.238	432.0	0.81
CS8	79.810±0.458	330.0	2.46
CS9	80.030±1.103	301.0	7.41

EE: Entrapment efficiency

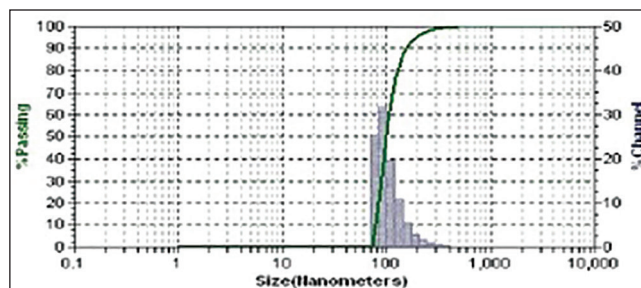


**Figure 1: Particle size analysis of batch CS5**

cubosome dispersion was observed under transmission electron microscope. The transmission electron micrographs show that the prepared cubosomes are in the nano-size, which confirms the results of particles size measurement. Micrographs show that the particles are cubic in shape, and well separated from each other. To confirm the formation of cubic structures in the prepared dispersions, the morphology was examined using cryo-TEM, and the obtained photomicrographs are presented in Figure 4.

### Characterization of Aloe vera hydrogel containing carbopol 934

All prepared *A. vera* hydrogel contains a different proportion of carbopol shows pH in the range of 6.3-6.5 which lies in the normal pH range of skin. Viscosity is one of the most important parameter as it affects the spreadability of the hydrogel. The viscosity of gel was dependent on polymer concentration, the batch HG3 shows optimum viscosity which may useful for pouring the dosage form on the wound as it can easily spread according to the shape of the wound. The addition of disodium EDTA was required to prevent a drop in viscosity during storage condition. Different *A. vera* hydrogel formulations were prepared with varying proportion of carbopol 934. The formulations were evaluated for pH, transparency, viscosity, and physical observation. The results are shown in Table 5. So, batch HG3 containing 1.5% of carbopol 934 was selected as optimized hydrogel base for cubosome dispersion due to its favorable characteristics such as transparency, homogeneity, smoothness, and gel formation.

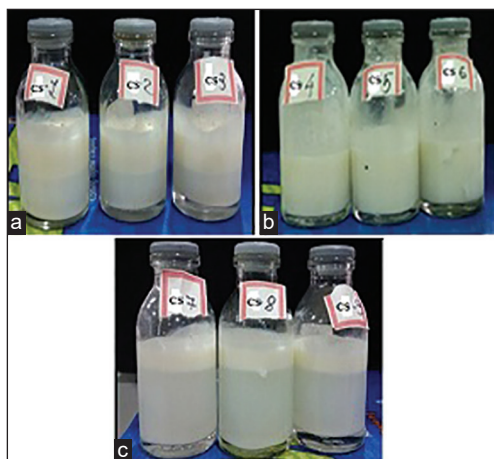


Figure 2: Cubosomes with (a) 0.5, (b) 1 and (c) 2 % of poloxamer 407

### Characterization of Aloe vera based silver sulfadiazine cubogel

#### Drug entrapment efficiency

Drug EE of all formulations is presented in Table 6. Under different ratios of GMO/P407, the EE was between 76% and 91%. The highest entrapment  $90.52 \pm 0.316$  was achieved at GMO/P407 ratio of 15/1 (CG3). At GMO/P407 ratios of 5/1 (CG1) and 10/1 (CG2), the EE was significantly lower than other ratios.

#### Bioadhesion measurement of Aloe vera based silver sulfadiazine cubogel

Bioadhesive properties of different cubosome loaded hydrogel were measured using physically modified balance. Figure 5 shows bioadhesive force of hydrogel without cubosome and bioadhesive force of different formulation. The results show that hydrogel without cubosome exhibited less bioadhesion as compared to cubosome loaded hydrogel may be due to the mucoadhesion property of cubogel.

#### Rheological properties of Aloe vera based silver sulfadiazine cubogel

The viscosity of prepared cubogels is displayed in Table 7. Rheological properties are important factors in the gel formulation and application, as they influence the product physical form, appearance, texture, and flow behavior.<sup>[39]</sup> It was found that all cubosome loaded hydrogel exhibited shear thinning flow [Figure 6] since the viscosity decreased with increasing shear rate.

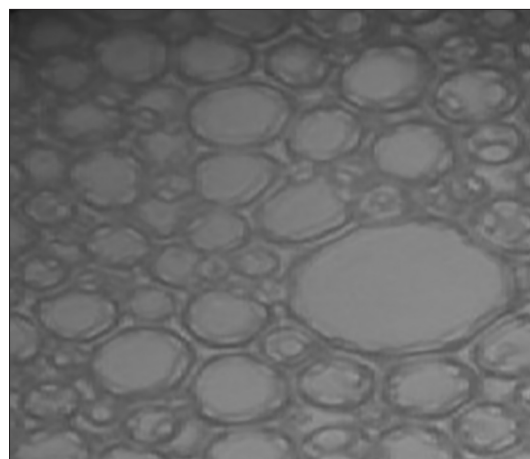


Figure 3: Optical micrograph of batch CG3 at magnification power of (a) ×400

**Table 5: Characterization of *A. vera* hydrogel containing carbopol 934**

Characterization	Batches			
	HG1	HG2	HG3	HG4
pH	6.3	6.4	6.5	6.4
Transparency	Transparent	Transparent	Transparent	Transparent
Viscosity (cps)	218.1	379.6	538.1	Very thick
Spread ability (s)	3.560	2.760	2.560	1.830
Physical observation	Thin gel, liquefy after 3 h	Thin gel, liquefy after 8 h	Uniform and smooth	Very thick and sticky

*A. vera*: Aloe vera

**In vitro diffusion study for drug release from Aloe vera based silver sulfadiazine cubogel**

*A. vera* based SSD cubogels (CG1-CG6 batch) prepared with a different proportion of GMO and P407 were subjected to *in vitro* drug release studied at pH 6.8 for 12 h using Franz diffusion cell. The cumulative percentage of SSD at different time intervals for each formulation is shown in Figure 7. The formulation CG1, CG4, CG5, and CG6 shows low diffusion (% cumulative drug release [CDR]) 76%, 85%, 82%, and 81%,

**Table 6: Percentage of EE of different formulations**

Formulations	EE (%)
CG1	76.36±0.340
CG2	80.47±0.429
CG3	90.52±0.316
CG4	85.41±0.515
CG5	82.52±0.886
CG6	80.45±0.823

EE: Entrapment efficiency

**Table 7: Viscosity of prepared cubogels at different speed**

Batches	Viscosity (cps) ± SD			
	10 rpm	20 rpm	50 rpm	100 rpm
CG1	925.0±1.769	793.7±2.100	558.2±2.672	401.7±3.583
CG2	926.9±1.665	746.5±3.074	487.1±2.023	328.5±1.386
CG3	927.3±0.862	803.5±1.969	695.0±2.311	549.9±0.611
CG4	929.1±0.814	812.8±2.165	614.7±1.700	503.1±4.823
CG5	975.0±5.655	802.1±0.901	503.6±3.041	427.7±0.416
CG6	981.5±0.945	832.5±1.539	620.9±1.517	564.2±1.040

SD: Standard deviation

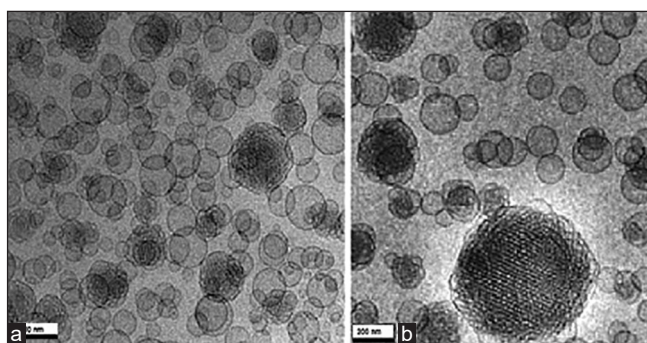


Figure 4: Cryo-transmission electron microscopic images of batch CG3 (a) Without drug, (b) Drug loaded

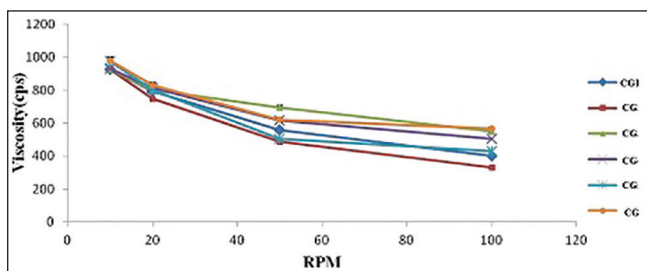


Figure 6: Rheograms of *Aloe vera* based silver sulfadiazine cubogel

respectively. The formulations CG2 and CG3 shows higher drug diffusion (% CDR) 93% and 98%, respectively. The result of % CDR shows that the different GMO content had a profound effect on drug release. A selection of optimized batch was done on basis of acceptance criteria. It was arbitrary decided to develop a formulation which releases 20% of drug in 1h and thereafter, the remaining amount of drug (i.e., 80%) should be released at constant rate of 7.27%/h. Based on this arbitrarily fixed criteria and an ideal release profile were decided, and batch CG3 was found to be optimum based on these criteria.

**Release kinetic study of Aloe vera based silver sulfadiazine cubogel**

In order to investigate the drug release kinetics, data were fitted to various kinetic models such as zero order, first order, Higuchi, Korsmeyer-Peppas, and Higuchi kinetic parameters, and correlation coefficient of each equation is presented in Table 8. It could be observed that the release of most *A. vera* based SSD cubogels follows diffusion controlled mechanism as also indicated from the highest coefficient of determination ( $R^2$ ).

**J flux calculation**

A formulation that shows higher flux is better than a formulation that shows lower flux. The flux value of all batches is shown in

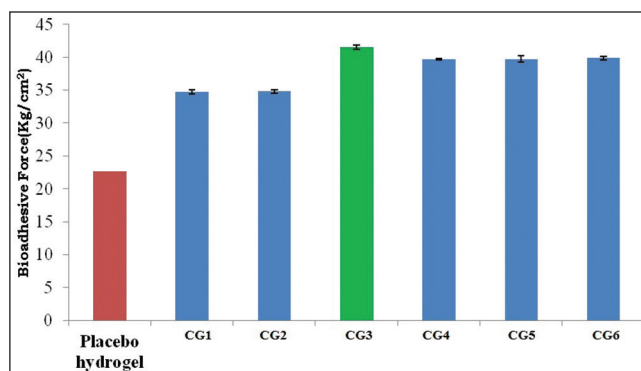


Figure 5: Comparative bioadhesive force of different formulations

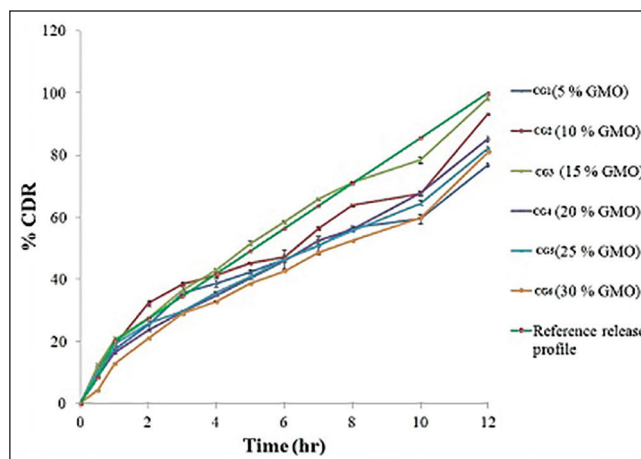


Figure 7: Comparative dissolution profiles of batches CG1-CG6 cubogels

Table 9. Batch CG3 shows highest flux (2.241 mg/cm<sup>2</sup>/h) and the highest permeation coefficient (0.074).

**Similarity factor**

The use of similarity factor ( $f_2$ ) has been endorsed by US FDA. The release profiles of all six batches (CG1-CG6) were compared with arbitrarily selected reference release profile. The computed values of similarity factor varied in between 44 and 77 as shown in Table 9. A value <50 indicate dissimilarity at 10% difference. Batches CG1, CG5, and CG6 have shown dissimilarity. Hence, the results of the remaining batches (CG2, CG4, and CG3) shall be examined for selection of optimum batch. Batches CG2 and CG4 showed similarity at marginal values. The batch CG3,

which shows similarity at <5% level ( $f_2 > 65$ ) and hence it may be considered as an optimum batch. The similarity factor covers the entire profile of drug release, it can be considered as a robust parameter. The batch CG3 was considered as optimum batch as it has optimized properties such as EE high (90%), complete and sustained drug release over 12 h, High bio-adhesive force (41 kg/cm<sup>2</sup>), and high permeability coefficient (0.074).

**In vivo study using animal model**

To estimate the wound healing effect of the cubogel for the acceleration of burn healing, the cubogels were applied to wound area in the rat dorsum. Figure 8 shows the macroscopic appearance of wounds treated with a cubogel without drug [Figure 8a], cubogel with SSD [Figure 8b], and SSD loaded *A. vera* based cubogel [Figure 8c], and marketed products [Figure 8d] at various days of postoperation. The cubogel without or with drugs was composed of 1.5 % carbopol 934 as a gelling agent and no drug, or 1% of the drug, respectively. Each wound was observed for a period of 2, 4, 6, 8, 10, and 12 days postoperation. All rats survived throughout the postoperative period. There was no evidence of necrosis. At the 2<sup>nd</sup> days postoperation, little inflammation was observed in all rats. The conventional product and the cubogels with and without drugs induced no infection, leads contraction of the wound, whereas the control group showed a hemorrhagic and scabbed wound spot. At 4<sup>th</sup> days postoperation, the control showed hemorrhage by second damage. In addition, re-epithelialization occurred more easily in other groups. From 6<sup>th</sup> days postoperation, the large portion of the wounds appeared to be healed and was mostly sealed. The relative size reduction of the wounds treated with different materials is illustrated in Figure 9. Till 4<sup>th</sup> days, there were no significant differences in wound size reduction. The hydrogel with and without SSD significantly decreased the wound size compared to the control from the 6<sup>th</sup> day of postoperation. Furthermore, from 08<sup>th</sup> days, the cubogel

**Table 8: Kinetic model data of each batch**

Batch	Zero order		First order		Higuchi model		Korsmeyer-Peppas	
	R <sup>2</sup>	Slope	R <sup>2</sup>	Slope	R <sup>2</sup>	Slope	R <sup>2</sup>	Slope
CG1	0.944	5.571	0.551	0.098	0.982	0.274	0.527	0.425
CG2	0.948	7.470	0.578	0.106	0.976	0.281	0.525	0.456
CG3	0.975	6.532	0.552	0.101	0.954	0.259	0.487	0.420
CG4	0.946	6.796	0.616	0.106	0.959	0.273	0.510	0.474
CG5	0.97	5.981	0.575	0.101	0.967	0.268	0.496	0.422
CG6	0.974	6.083	0.652	0.115	0.955	0.275	0.537	0.604

**Table 9: Results of J flux, permeability coefficient, and similarity factor**

Batches	J flux (mg/cm <sup>2</sup> /h)	Permeability coefficient	f <sub>2</sub> value (similarity factor)
CG1	1.671±0.040	0.057	47.85
CG2	1.959±0.010	0.065	56.11
CG3	2.240±0.007	0.074	77.27
CG4	1.918±0.015	0.064	50.59
CG5	1.794±0.005	0.059	49.19
CG6	1.829±0.003	0.061	44.01

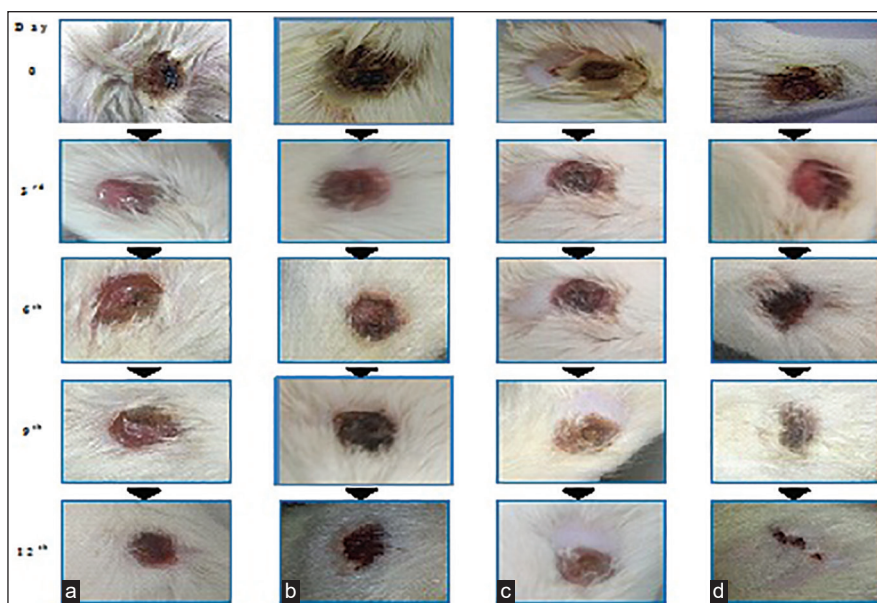


**Figure 8:** In vivo burn healing study. (a) Cubogel without the drug. (b) Marketed preparation. (c) Cubogel containing silver sulfadiazine (d) cubogel containing silver sulfadiazine and *Aloe vera* at the end of 0, 3<sup>rd</sup>, 6<sup>th</sup>, 9<sup>th</sup>, and 12<sup>th</sup> days



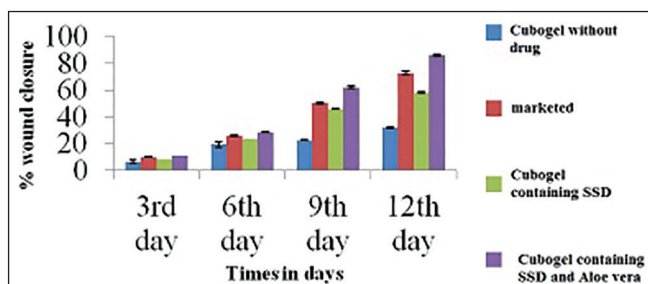


**Figure 9:** Comparison of % burn wound contraction of cubogel with marketed product, placebo cubogel and with control

with and without drugs showed a significantly greater wound size reduction than the conventional product did. After the 10<sup>th</sup> days postoperation, there was complete healing occurred in the *A. vera* based SSD cubogel with the formation of natural skin, while 70-80% healing occurred in cubogel with SSD and both has faster healing as compared to marketed preparation.<sup>[42,46-49]</sup> *In vivo* wound, healing study revealed that the cubogel with drug and *A. vera* shows no scar formation after healing because of antiscarring effect of *A. vera* and generate normal skin without scarring.<sup>[50]</sup> In marketed formulation, the pseudoeschar formed during the healing which hindered the permeation of drug so delay in healing and sometimes leading to infection in the wound. So cubogel shows greater healing than marketed product. Thus, the prepared SSD and *A. vera* loaded Cubogel significantly improves the burns healing and possible hopes for the severe burns and burn infection.

**Histopathological examination**

Photomicrographs of histopathological sections representing skin of rats of different groups after 2<sup>nd</sup>, 4<sup>th</sup>, and 12<sup>th</sup> day are presented in Figure 10: (a) cubogel without drug: After 12 days, there was focal necrosis as well as regeneration of the epidermis associated with massive number of inflammatory cells infiltration in the underlying dermal tissue. Newly formed blood capillaries with inflammatory cells infiltration were detected in the deep subcutaneous and dermal tissues. Form the above, it can be observed that inflammation and granulation tissue was not formed until day 12, (b) Optimized cubogel with SSD: Regeneration of epidermis started on day 6. After 12 days, complete regeneration was detected in the epidermis associated with granulation tissue formation and few inflammatory cells infiltration in the underlying dermal and subcutaneous tissues, (c) Optimized cubogel with SSD + *A. vera*: Regeneration in epidermis and granulation tissue formation started on day 2, and fibrosis occurred on day 6 with the complete regeneration of epidermis at day 12. These are the best results in comparison with other test groups and commercial product group, and (d) Marketed product: Inflammation and necrosis lasted until day 6 because of the cream base effect. Granulation tissue formation and fibrosis started at day 12, and regeneration of epidermis was not completed because of cytotoxicity of SSD to fibroblasts.

**Stability study of optimized formulation**

The stability study was carried out on the optimized formulation.<sup>[43,44]</sup> The results of stability testing are depicted in Table 10. The

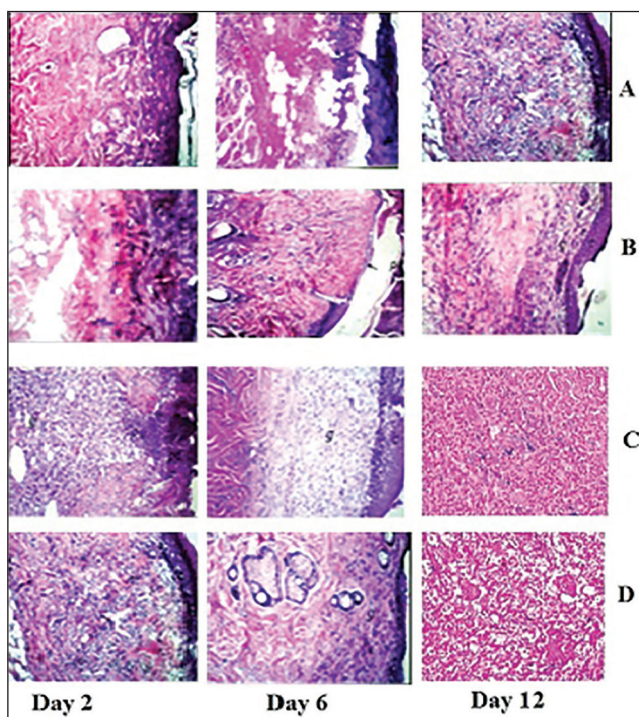


**Figure 10:** Photomicrographs of histopathological sections representing burned skin of rat groups following treatment for 12 days, cubogel without drug (a), Optimized cubogel with silver sulfadiazine (b), Optimized cubogel with silver sulfadiazine + *Aloe vera* (c), And marketed product (d)

**Table 10: Stability testing data of optimized batch**

Days	EE (%)	pH	Viscosity (cps)	Physical appearance
0	90.06±1.25	6.8±0.03	928.4±0.38	White milky
5	89.92±0.56	6.8±0.03	928.1±1.47	White milky
15	89.85±1.30	7.0±0.04	927.8±0.73	White milky
20	89.73±2.12	7.0±0.02	927.8±0.81	White milky
30	88.13±0.85	7.0±0.01	927.1±1.51	White milky

EE: Entrapment efficiency

formulations were stored at 40 ± 2°C/75 ± 5% RH for 1-month to assess their accelerated stability. After an interval of 5, 10, 15, 20, and 30 days, samples were withdrawn and retested for % of EE, pH, viscosity, and physical appearance. Significant changes in % of EE, viscosity, pH, and physical appearance of cubogel were not noticed. This result indicates that formulations remained stable for 1-month under accelerated conditions.

**CONCLUSION**

In the present study, cubogel containing SSD and *A. vera* were successfully developed for severe burns wound condition. Results in this study shows that the formulation of cubosome dispersions containing SSD in cubic liquid crystalline nanoparticles provides controlled release of SSD hence avoiding the cytotoxic effect of silver. Formulating SSD cubosomes with *A. vera* into cubogels using poloxamer 407 enabled the enhancement of burn healing

and overcoming the disadvantages of the current commercial carrier base. It has the ability to be applied from the 1<sup>st</sup> day of burn without affecting the healing process because it's miscibility with biological fluid and the antimicrobial and antiscar properties of *A. vera*. Healing of tissues started earlier than marketed product. SSD cubogel formula containing cubosome dispersion CG3 (15% GMO, 1% poloxamer 407, *A. vera* gel), and 1.5 % carbopol 934, could hence be used very successfully in the management of deep second degree burn leading to excellent healing results with least side effects in comparison with most of the formulations present in the market, hence better patient compliance.

### Financial support and sponsorship

Nil.

### Conflicts of interest

There are no conflicts of interest.

## REFERENCES

- Available from: [http://www.who.int/violence\\_injury\\_prevention/other\\_injury/burns/en/](http://www.who.int/violence_injury_prevention/other_injury/burns/en/) [Last accessed on 2014 Mar 7]
- Atiyeh BS, Costagliola M, Hayek SN, Dibo SA. Effect of silver on burn wound infection control and healing: Review of the literature. *Burns* 2007;33:139-48.
- Greenhalgh DG. Topical antimicrobial agents for burn wounds. *Clin Plast Surg* 2009;36:597-606.
- Brittain H. Analytical Profiles of Drug Substances. San Diego: Academic Press; 2001.
- Parashar P. Synthesis of silver nanocomposite with poly(vinylpyrrolidone) and poly(4-vinylpyridine) for antimicrobial activity. *Adv Mat Res* 2013;772:9-14.
- Heggors J, Richard J, Spencer B, McCoy L, Carino E, Washington J, et al. Acticoat versus silverlon: The truth. *J Burn Care Rehabil* 2002;23:S115.
- Hayden DM, Forsyth C, Keshavarzian A. The role of matrix metalloproteinases in intestinal epithelial wound healing during normal and inflammatory states. *J Surg Res* 2011;168:315-24.
- Gear AJ, Hellewell TB, Wright HR, Mazzaresse PM, Arnold PB, Rodeheaver GT, et al. A new silver sulfadiazine water soluble gel. *Burns* 1997;23:387-91.
- Montagna W. *Advances in Biology of Skin*. Oxford: Symposium Publications Division, Pergamon Press; 1960.
- Muller MJ, Hollyoak MA, Moaveni Z, Brown TL, Herndon DN, Heggors JP. Retardation of wound healing by silver sulfadiazine is reversed by *Aloe vera* and nystatin. *Burns* 2003;29:834-6.
- Cooper ML, Laxer JA, Hansbrough JF. The cytotoxic effects of commonly used topical antimicrobial agents on human fibroblasts and keratinocytes. *J Trauma* 1991;31:775-82.
- McCauley RL, Linares HA, Pelligrini V, Herndon DN, Robson MC, Heggors JP. *In vitro* toxicity of topical antimicrobial agents to human fibroblasts. *J Surg Res* 1989;46:267-74.
- Dunn K, Edwards-Jones V. The role of Acticoat with nanocrystalline silver in the management of burns. *Burns* 2004;30 Suppl 1:S1-9.
- Tsuruta T. *Biomedical Applications of Polymeric Materials*. Boca Raton: CRC Press; 1993.
- Peppas NA, Bures P, Leobandung W, Ichikawa H. Hydrogels in pharmaceutical formulations. *Eur J Pharm Biopharm* 2000;50:27-46.
- Bhattarai N, Gunn J, Zhang M. Chitosan-based hydrogels for controlled, localized drug delivery. *Adv Drug Deliv Rev* 2010;62:83-99.
- Hoffman AS. Hydrogels for biomedical applications. *Ann N Y Acad Sci* 2001;944:62-73.
- Drummond C, Fong C. Surfactant self-assembly objects as novel drug delivery vehicles. *Curr Opin Colloid Interface Sci* 1999;4:449-56.
- Almgren M. Vesicle transformations resulting from curvature tuning in systems with micellar, lamellar, and bicontinuous cubic phases. *J Dispers Sci Technol* 2007;28:43-54.
- Schwarz J, Contescu C, Putyera K. *Dekker Encyclopaedia of Nanoscience and Nanotechnology*. New York: M. Dekker; 2004.
- Sadhale Y, Shah JC. Stabilization of insulin against agitation-induced aggregation by the GMO cubic phase gel. *Int J Pharm* 1999;191:51-64.
- Sadhale Y, Shah JC. Biological activity of insulin in GMO gels and the effect of agitation. *Int J Pharm* 1999;191:65-74.
- Almgren M, Rangelov S. Polymorph dispersed particles from the bicontinuous cubic phase of glycerol monooleate stabilized by PEG-copolymers with lipid-mimetic hydrophobic anchors. *J Dispers Sci Technol* 2006;27:599-609.
- Bunyaphatsara N, Jirakulchaiwong S, Thirawarapan S, Manonukul J. The efficacy of *Aloe vera* cream in the treatment of first, second and third degree burns in mice. *Phytomedicine* 1996;2:247-51.
- Khan AW, Kotta S, Ansari SH, Sharma RK, Kumar A, Ali J. Formulation development, optimization and evaluation of *Aloe vera* gel for wound healing. *Pharmacogn Mag* 2013;9 Suppl 1:S6-10.
- Esposito E, Eblovi N, Rasi S, Drechsler M, Di Gregorio GM, Menegatti E, et al. Lipid-based supramolecular systems for topical application: A preformulatory study. *AAPS PharmSci* 2003;5:E30.
- Kwon T, Hong S, Kim J. *In vitro* skin permeation of cubosomes containing triclosan. *J Ind Eng Chem* 2012;18:563-7.
- Esposito E, Cortesi R, Drechsler M, Paccamiccio L, Mariani P, Contado C, et al. Cubosome dispersions as delivery systems for percutaneous administration of indomethacin. *Pharm Res* 2005;22:2163-73.
- Esposito E, Ravani L, Mariani P, Huang N, Boldrini P, Drechsler M, et al. Effect of nanostructured lipid vehicles on percutaneous absorption of curcumin. *Eur J Pharm Biopharm* 2014;86:121-32.
- Gan L, Han S, Shen J, Zhu J, Zhu C, Zhang X, et al. Self-assembled liquid crystalline nanoparticles as a novel ophthalmic delivery system for dexamethasone: Improving precocular retention and ocular bioavailability. *Int J Pharm* 2010;396:179-87.
- Esposito E, Cortesi R, Drechsler M, Paccamiccio L, Mariani P, Contado C, et al. Cubosome dispersions as delivery systems for percutaneous administration of indomethacin. *Pharm Res* 2005;22:2163-73.
- Esposito E, Ravani L, Contado C, Costenaro A, Drechsler M, Rossi D, et al. Clotrimazole nanoparticle gel for mucosal administration. *Mater Sci Eng C Mater Biol Appl* 2013;33:411-8.
- Thapa RK, Yoo BK. Evaluation of the effect of tacrolimus-loaded liquid crystalline nanoparticles on psoriasis-like skin inflammation. *J Dermatolog Treat* 2014;25:22-5.
- Esposito E, Ravani L, Mariani P, Contado C, Drechsler M, Puglia C, et al. Curcumin containing monoolein aqueous dispersions: A preformulative study. *Mater Sci Eng C Mater Biol Appl* 2013;33:4923-34.
- Sauzet C, Claeys-Bruno M, Nicolas M, Kister J, Piccerelle P, Prinderre P. An innovative floating gastro retentive dosage

- system: Formulation and *in vitro* evaluation. *Int J Pharm* 2009;378:23-9.
36. Purohit S, Solanki R, Soni M, Mathur V. Experimental evaluation of Indian *Aloe (Aloe Vera)* leaves pulp as topical medicament on wound healing. *Int J Pharmacol Res* 2012;2:4-12.
  37. Niamlang S, Buranut T, Niansiri A. Electrically controlled *Aloe-Vera* extraction release from poly acrylamide hydrogel. *Energy Procedia* 2011;9:468-73.
  38. Sahoo S, Pani NR, Sahoo SK. Microemulsion based topical hydrogel of sertaconazole: Formulation, characterization and evaluation. *Colloids Surf B Biointerfaces* 2014;120:193-9.
  39. Worachun N, Opanasopit P, Rojanarata T, Ngawhirunpat T. Development of ketoprofen microemulsion for transdermal drug delivery. *Adv Mat Res* 2012;506:441-4.
  40. Shah R, Patel D, Mehta M, Patel C. Design and optimization of mucoadhesive nasal *in situ* gel containing sodium cromoglycate using factorial design. *Asian J Pharm* 2011;5:65-8.
  41. Singh V, Pramanik K, Ray S, Pal K. Development and characterization of sorbitan monostearate and sesame oil-based organogels for topical delivery of antimicrobials. *AAPS PharmSciTech* 2014;8:5-13.
  42. Patel NV, Patel JK, Shah SH. Box-Behnken experimental design in the development of pectin-compritol ATO 888 compression coated colon targeted drug delivery of mesalamine. *Acta Pharm* 2010;60:39-54.
  43. Balakrishnan B, Mohanty M, Umashankar PR, Jayakrishnan A. Evaluation of an *in situ* forming hydrogel wound dressing based on oxidized alginate and gelatin. *Biomaterials* 2005;26:6335-42.
  44. Nilani P, Pranavi A, Duraisamy B, Damodaran P, Subhashini V, Elango K. Formulation and evaluation of wound healing dermal patch. *Afr J Pharm Pharmacol* 2011;5:1252-7.
  45. Bancroft J, Gamble M. Theory and practice of histological techniques. Philadelphia, PA: Churchill Livingstone/Elsevier, 2008. 6<sup>th</sup> Ed.
  46. Gordon S, Young K, Wilson R, Rizwan S, Kemp R, Rades T, *et al.* Chitosan hydrogels containing liposomes and cubosomes as particulate sustained release vaccine delivery systems. *J Liposome Res* 2012;22:193-204.
  47. Sung JH, Hwang MR, Kim JO, Lee JH, Kim YI, Kim JH, *et al.* Gel characterisation and *in vivo* evaluation of minocycline-loaded wound dressing with enhanced wound healing using polyvinyl alcohol and chitosan. *Int J Pharm* 2010;392:232-40.
  48. Davis RH, Donato JJ, Hartman GM, Haas RC. Anti-inflammatory and wound healing activity of a growth substance in *Aloe vera*. *J Am Podiatr Med Assoc* 1994;84:77-81.
  49. Shelton RM. *Aloe vera*. Its chemical and therapeutic properties. *Int J Dermatol* 1991;30:679-83.
  50. Davis RH, DiDonato JJ, Johnson RW, Stewart CB. *Aloe vera*, hydrocortisone, and sterol influence on wound tensile strength and anti-inflammation. *J Am Podiatr Med Assoc* 1994;84:614-21.